How Many Rubble Piles Are in the Asteroid Belt?

A Campo Bagatin, Jean-Marc C. Petit

How Many Rubble-Piles in the Asteroid Belt?

A. Campo Bagatin, J–M. Petit

Observatoire de la Côte d'Azur, Nice, France

and

P. Farinella *

Dipartimento di Astronomia, Università di Trieste, Italy

petit@obs-nice.fr

length:

40 manuscript pages

1 table

9 figures

---

*Died on March 25th, 2000, from the result of heart disease. He was the one who introduced us to the physics of collisions and the collisional evolution of Asteroids. This paper is dedicated to his memory.

Proposed running title: How Many Rubble-Piles in the Asteroid Belt?

Send proofs to:

Jean-Marc Petit
Observatoire de la Côte d'Azur
B.P. 4229
F-06304 Nice Cedex 4 France

Tel: +33 4 92 00 30 89
Fax: +33 4 92 00 30 33
Internet: petit@obs-nice.fr

Abstract

We have developed a new version of the code built by Campo Bagatin *et al.* , 1994a,b and Campo Bagatin, 1998 to model the collisional evolution of the asteroid size distribution. The new code distinguishes between "intact", unfractured asteroids that did not undergo catastrophic collisions, and asteroids converted by energetic collisions into reaccumulated bodies, or "rubble–piles". The distinction can also be made on a physical ground, by assigning different collisional parameters to the two kinds of objects, with the objective of simulating the different responses to energetic impacts that rubble–piles may have – due to their different structure – in comparison to unshattered bodies. Rubble–piles abundance turns out to be generally higher when such targets are supposed to transfer less kinetic energy to the fragments than monolithic asteroids.

We have run a number of simulations of the collisional evolution process to assess the size range where reaccumulated bodies should be expected to be abundant in the main asteroid belt. We find that this diameter range goes from about 10 to 100 km, but may extend to smaller or larger bodies depending on the prevailing collisional response parameters, such as the strength of the material, the strength scaling law, the fraction of kinetic energy of the impact transfered to the fragments and the reaccumulation model.

Both the size range and the resulting fraction of rubble–piles vary widely depending on the input parameters. This reflect the large uncertainties still present in the modelisation of high velocity impact outcomes. In particular, the simulations that take into account the derived "hydrocode" scaling laws (Davis *et al.* , 1994) show that nearly 100% of the main belt asteroids larger than a few kms should be reaccumulated objects. On the other hand the present code shows that the scaling–law recently proposed by Durda *et al.* , 1998 produces almost no rubble–pile. This scaling–law was proposed to match the actual population of asteroids which it fails to do if collisional processes are accounted for in a self–consistent way.

I   Introduction

Due to the large number of objects and the non–negligible orbital eccentricities and inclinations, the asteroid belt population forms a collisional system. Typical collision velocities are of the order of 5 km/s (Farinella and Davis, 1992, Bottke *et al.* , 1994, Vedder, 1997) in the main belt, and at these speeds a wide range of collisional outcomes is possible (Davis *et al.* , 1989, Petit and Farinella, 1993). We refer to Campo Bagatin *et al.* , 1994a,b and especially to Campo Bagatin, 1998 for an introduction and a review of asteroid belt physical and collisional issues.

In monolithic asteroidal impacts, there is an energy threshold beyond which localized target damage associated with cratering events gives way to global shattering and target breakup. In the latter case, the ejection velocity of the fragments

may either be large enough to allow all (or most) of them to escape "to infinity" with independent heliocentric orbits, or conversely may be so low that most (or all) of the fragments fall back and are reaccumulated into a gravitationally bound "rubble–pile".

Recent years' space probes and radar observations of asteroids such as Mathilde and Eros (NEAR probe), Gaspra and *Ida* (Galileo probe), Castalia, Toutatis and *1999JM8* (radar observations) are throwing new light into the previously poorly known structures of asteroids. The characteristics of some of these bodies suggest that they can be reaccumulated bodies; peculiar features such as the presence of enormous crater basins, about half the size of the body itself, in the case of Mathilde, suggest that the collisional response to energetic impacts may be different compared to monolithic objects. In fact, rubble–piles may be less efficient than unshattered objects in delivering kinetic energy of impacts to external fragments (Asphaug *et al.* , 1998), due to some reasons that will be explained in Sec. III.

The reaccumulation process may be complicated by the existence of a correlation between velocity and mass of the ejected fragments. Some evidence of such a correlation has been found in the past from laboratory experiments (Nakamura & Fujiwara, 1991; Nakamura *et al.* , 1992; Giblin *et al.* , 1994; Giblin, 1998). The experimental results actually show a large dispersion in the data, and the slope of the tentative linear fit matching them has to be considered with caution when considering a schematic mathematical correlation to display the phenomenon. In fact, simplifying the "dispersed" mass–velocity correlation, i.e. velocity spread over a large range of values for any given mass, with a well-defined, straight power–law relationship may yield in some case to misleading results, as will be shown in Sec. IV.A and IV.B.

Anyway, this is potentially an important finding, because such a correlation would strongly affect the extent to which reaccumulation is effective in creating a "shoulder" in the collisionally evolved size distribution (Campo Bagatin *et al.* , 1994b) or determining the internal structure of the resulting rubble–pile objects (Wilson *et al.* , 1999) and the amount of material falling back after a shattering event. Recent data, however, indicate that the velocity–mass correlation may be weaker or stronger—depending on the material properties—than assumed earlier, and possibly depending on the specific impact conditions or the experimental setup (Giblin, 1998).

Another possible complicating factor is that non–disruptive cratering events may also create a deep layer of regolith (fragmented material) and thus favour the transformation of intact asteroids into rubble–piles. However, quantitative estimates (e.g. Farinella *et al.* , 1993) show that the crater ejecta accumulated over an asteroid's lifetime typically account for only a small fraction of the total mass.

Here, we shall report the numerical results that we have obtained on the abundance of rubble–pile asteroids in the main belt population, as a function of size and of some poorly known collisional response parameters. Hopefully, future data on the outcomes of hypervelocity impacts, the internal structure of asteroids and their size distribution as a function of material type will further constrain our models.

In Sec. II, an outline of the numerical models performing the simulations of

the collisional evolution is given, together with a description of the scaling laws that have been used, and of the models of reaccumulation considered in the fragmentation code. The definition of "rubble-pile" is given in Sec. III, and a discussion on the possible physical differences existing between these kind of bodies and monolithic bodies is also included. The results of various simulations are shown and explained in Sec. IV. Finally, some conclusions are drawn from the results of the whole set of simulations performed in this work and are presented in Sec. V.

II   Numerical Model

The aim of the present work is to give an estimate of the abundance of reaccumulated asteroids in the main belt as a function of their size, taking into account the dependence on various physical effects and modelling assumptions. For this purpose, we have developed a new version of the numerical evolution model described in Campo Bagatin *et al.* , 1994a,b. This code simulates the collisional history of asteroids by evolving in time the populations of objects residing in a set of N_{bin} discrete size bins (usually 60), integrating numerically a set of N_{bin} non–linear, first–order differential equations. From one bin to the next one, the mass of the bodies changes by a factor of 2, i.e. the diameter changes by a factor of $2^{1/3}$. In the original version of the code, at any time step the expected number of collisions between bodies belonging to any pair of bins is computed, and in each case a collisional outcome algorithm provides the size distribution of the objects resulting from the impacts, which are then redistributed into the size bins. In the current version, the collisional algorithm also records the kind of outcome occurring in each case (*cratering, reaccumulation* or *disruption*, with the latter term denoting breakup without reaccumulation) and separates the resulting bodies into reaccumulated objects and "single" fragments. This allows us to compute, in any size bin, the fraction of reaccumulated bodies over the total population, and how this fraction evolves with time (we assume that at the beginning of the evolution it is zero).

The collisional outcome algorithm works in the following way. For each colliding body the available impact energy E per unit volume V is compared to a fragmentation threshold S (the *impact strength*), which is assumed to scale with size according to two different effects: a gravitational self–compression effect as suggested by Davis *et al.* , 1985 and Housen *et al.* , 1991, and a strain–rate effect (Housen and Holsapple, 1990). The latter effect decreases the strength for increasing sizes, until the former takes over and makes large bodies stronger and stronger (Davis *et al.* , 1994). In absence of well established data, and to make things simple, we neglect any dependence of the imapct strength on the impact velocity. When the available energy exceeds the threshold, this corresponds to a *shattering* event, where the mass of the largest intact fragment is less than half the mass of the target. Otherwise, it is a *cratering* event. We have considered three main scaling laws, basically the ones summarized in Davis *et al.* , 1994, that we report here for the sake of completeness.

Energy scaling:

$$S = S_0 + \frac{4\pi\alpha G\rho^2 R^2}{15} \tag{1}$$

Strain rate scaling:

$$S = S_0 \left(\frac{R}{10cm}\right)^{-0.24} \left[1 + 2.14 \times 10^{-11}\alpha\left(\frac{R}{10cm}\right)^{1.89}\right] \tag{2}$$

Hydrocode–basalt:

$$S = S_0 \left(\frac{R}{10cm}\right)^{-0.43} \left[1 + 1.07 \times 10^{-17}\alpha\left(\frac{R}{10cm}\right)^{3.07}\right] \tag{3}$$

S_0 is the *material strength*, as measured by laboratory experiments, α is the so–called *self–compression* coefficient, G the gravitational constant, ρ the material density, R the target radius. Figure 1 shows the variation of S as a function of the radius of the target R. Here, as well as in all our simulations, we have assumed a value of the self–compression coefficient $\alpha = 100$. For the energy scaling and the strain–rate scaling, $S_0 = 3 \cdot 10^6$ J/m^3, while for the hydrocode scaling, $S_0 = 8.22 \cdot 10^6$ J/m^3.

Note that some authors prefer to consider the *specific energy*—that is the energy per unit mass (Q_S^*, or simply Q^*)—for shattering, instead of the strength; it's worth recalling that these two quantities are related by the following simple relationship: $Q^* = S/\rho$.

The behaviour of the three scaling laws written above are displayed together with the scaling law proposed by Durda *et al.* , 1998, in Fig. 1.

The *energy–scaling* for the strength was formerly proposed by Davis *et al.* , 1985, who just accounted for gravitational self–compression, without any *strain–rate* effect. As can be seen in Fig. 1, for a given material the strength is constant for any body of size smaller (*strength* regime) than the size at which the gravity scaling increases the value of the strength. After a transition range, the strength keeps on steadily increasing with size (*gravity* regime).

In the case of *strain–rate scaling*, we used two different exponents: the nominal value 0.24, that can be found in Eq. 2, and 0.33. The first one refers to what Housen *et al.* , 1991 report, the second one is to follow more recent calculations (Holsapple, 1994). This exponent has been given different values in the last two decades. Fujiwara, 1980, and independently, Farinella *et al.* , 1982 suggested the 0.5 value, that meant a marked dependence of strain–rate effects on size, large objects – below the gravity regime – should have then been very weak. Later scaling theories performed by Housen *et al.* , 1991 suggested a much shallower value for this dependence (0.24). In recent years, both hydrocodes and revisited scaling theories are suggesting again a higher value for this exponent (0.33, Holsapple, 1994; 0.43, Davis *et al.* , 1994; 0.59, 0.667, Housen and Holsapple, 1999).

The *hydrocode–scaling* instead is a recently derived scaling law, inferred from hydrocode simulations of fragmentation processes (Davis *et al.* , 1994)), it depends on the properties of different materials and has a strong dependence of strain–rate

scaling on size, namely a decrease of 2–3 orders of magnitude between 10 cm and 25 km.

We also report here a recently proposed scaling law (Durda *et al.* , 1998), that was argued to match the actual distribution of asteroids in the main belt, if inserted in the present fragmentation and collisional evolution codes. We checked that scaling law with our self–consistent fragmentation code and we anticipate here that the final size distribution does not fit the observations, mainly because of inconsistencies in Durda *et al.* model (see Sec. IV.F).

Once the comparison between the impact energy per unit volume and the value of S is made, the impact may happen to be either a cratering event, or a fragmentation event. In both cases the size distribution of the created fragments is calculated. See Petit and Farinella, 1993 and Campo Bagatin, 1998 for a detailed presentation of the fragmentation model. The critical quantity that discriminates cratering from shattering is the mass fraction between the largest remnant (M_{LR}) and the target (M_T), which is given by:

$$f_{LR} = \frac{M_{LR}}{M_T} = 0.5 \left[\frac{S M_T}{\rho(E_K/2)} \right]^{1.24} \tag{4}$$

in the case of shattering $f_{LR} \leq 0.5$.

As for the reaccumulation process, we have followed Campo Bagatin *et al.* , 1994b in adopting two different models.

a) A "mass–velocity" model (Petit and Farinella, 1993), *PF model* in what folows, that assumes that there is a weak power–law correlation between the mass and velocity of fragments ejected in a catastrophic collision, according to the experimental results mentioned in Sec. I. The general aspect of the relationship between mass m and velocity V that we adopted in our nominal case is

$$V \propto M^{-r}. \tag{5}$$

The value of exponent r has been found to be about 1/6 by Nakamura and Fujiwara, 1991, or to be in between 0 and 1/6, with a mean value of 1/13 (Giblin, 1998), with a considerable dispersion of data around the proposed slopes. Any fragment with velocity larger than the escape velocity V_{esc}, derived from the gravitational potential of the two colliding bodies, will escape, while those slower than V_{esc} will reaccumulate on the largest remnant. In this model, a given mass corresponds to a single velocity.

b) A so–called "cumulative" model, in which no correlation between mass and velocity of fragments is considered. In this case, the velocity distribution is the same for all fragment mass and the fraction of mass with a velocity larger than V is

$$f(> V) \equiv \frac{M(> v)}{M_T} = \left(\frac{V}{V_{min}} \right)^{-k}, \tag{6}$$

where k is a given exponent, larger than 2 (to allow for conservation of energy), and generally assumed to be $k \approx 9/4$, and V_{min} is a lower cutoff for the velocity of fragments. By integrating over v between v_{min} and ∞ we obtain the total kinetic

7

energy of the ejected fragments E_{fr}. Hence:

$$V_{min} = \sqrt{\frac{k-2}{k}\frac{E_{fr}}{M_T}}. \tag{7}$$

The kinetic energy of the fragments is a given fraction of the impact kinetic energy deposited in the target $E_K/2$:

$$E_{fr} = f_{KE}\frac{E_K}{2}. \tag{8}$$

This model assumes that in each mass bin, there are fragments with velocity larger than V_{esc}, which would escape. The fraction of such fragments is $f(>V_{esc})$. The other ones are reaccumulated on the largest remnant.

The above defined f_{KE} is a poorly known parameter in collisional processes. Laboratory experiments suggest values of the order of 0.01, while in order to be able to reproduce the formation of asteroid families this value is constrainted to be of the order of 0.1. It may even vary with size and probably with impact speed. In the simulation presented in Sec. IV.F, we define f_{KE} as a function of the target size. The situation seems to be more complex in the case of reaccumulated objects, as discussed in Sec. III.

The three scaling laws previously described have been derived from physical considerations. We also tested the scaling law proposed by Durda *et al.* , 1998, which was derived by fitting the observed size distribution of asteroids with the results of their model. We used the parameters from their fit 1. The quantity derived by Durda *et al.* is Q_D^*, the specific energy for dispersal, i.e. $M_T Q_D^*$ is the minimum kinetic energy of the projectile required to disperse at least half the mass of the target, accounting for potential reaccumulation. From their numbers, we get:

$$Q_D^* = 1.1445 \cdot 10^{-7} D^{1.028} e^{\left(5.932 \cdot 10^{-6} \sqrt{8.895\ 10^{12} + 6.586\ 10^{10}\ \ln(D) + 2.466\ 10^{11}\ \ln(D)^2}\right)}, \tag{9}$$

where $D = 2R$. In our collisional model, we consider the specific energy required to shatter the target, Q_S^*. Reaccumulation is accounted for subsequently, by the specification of the fraction of kinetic energy given to the fragments (f_{KE}) and the velocity distribution (PF or cumulative). How are Q_D^* and Q_S^* related ?

As a first step, let us derive the relationship between Q_D^* and f_{KE}. Here we assume a cumulative velocity distribution (Eq. 6). Since dispersal is defined by $f(>v_{esc}) > 1/2$, from Eq. 6 we obtain that for the critical collision corresponding to Q_D^*, $v_{min} = 2^{-1/k} v_{esc}$. We recall that Q_D^* is the minimum projectile energy required for target dispersal, assuming that $1/2$ of the projectile energy E_K is delivered to the target and that a fraction f_{KE} of this is partitioned into kinetic energy of fragments. Thus, for the critical collision corresponding to Q_D^* we have:

$$f_{KE} = \frac{2E_{fr}}{M_T Q_D^*} = \frac{k}{k-2}\ 2^{-2/k}\ \frac{v_{esc}^2}{Q_D^*}, \tag{10}$$

Following Durda and Dermott, 1997 (their Eq. 7), we define the minimum energy to disperse a given target as the sum of the energy needed to shatter the body and the energy required to disperse the fragments:

$$E_K = Q_D^* \, M_T = \frac{Q_S^* \, M_T}{f_{SH}} + \frac{1}{f_{KE}} \, 0.411 \, \frac{2 \, G \, M_T^2}{D}. \tag{11}$$

Here, we introduce f_{SH} which is the fraction of kinetic energy of the projectile used to shatter the target, assumed to be 1/2 in our work, while Durda and Dermott used $f_{SH} = f_{KE}$. In Eq. 10, for consistency with Eq. 11 and Durda and Dermott, we use:

$$V_{esc}^2 = 0.822 \frac{4 G M_T}{D}. \tag{12}$$

This yields:

$$Q_S^* = f_{SH} \left[Q_D^* - \frac{1}{f_{KE}} \, 0.411 \, \frac{2 \, G \, M_T}{D} \right] = f_{SH} \, Q_D^* \left[1 - \frac{k-2}{k} \, 2^{2/k} \, \frac{1}{4} \right]. \tag{13}$$

Figure 1 shows the value of $S_{Durda} = Q_S^* \rho$ as a function of R, using $\rho = 2500$ kg/m^3, as in all our simulations.

Once the outcome of the impacts between any given pair of asteroids is calculated, the results are plugged into the collisonal evolution model, as mentioned above.

Campo Bagatin *et al.* , 1994a, and Campo Bagatin, 1998, showed that in a collisional system with a sharp cutoff at small sizes, a perturbation to the stationary distributions arises in form of "waves", that is oscillations about the steady state power law distribution found by Dohnanyi, 1969. To avoid this "wave" effect, we do not evolve the smaller mass bins that would directly be influenced by the cutoff with the general algorithm. Instead, we force those bins (typically the 15 smaller mass bins) to follow a power law distribution, the exponent of which is the average power law exponent of the next 10 bins. In this way, the bins that evolve according to the general algorithm always have an appropriate set of projectiles and then do not exhibit the wave pattern. If the number of constrainted bins is decreased, we may see a wave develop. If it is increased, nothing changes, but this increase the computational requirement. Due to this forcing of the number of bodies in the small size bins, there is a change in mass. But it is negligeable due to the rather shallow size distrbution at small sizes, the mass being in the large bodies.

III About "Rubble–Piles"

The existence of asteroid rubble–piles is both possible and probable. It is possible because from a theoretical point of view it is clear that such objects may form; on the other hand, many authors have suggested such bodies to explain features of comets and asteroids compositions (Weissman, 1986, Asphaug and Benz, 1994, Melosh and Ryan, 1997, Whipple, 1998, Wilson *et al.* , 1999). And it is now also probable that rubble–piles exist; observations of the late comet Shoemaker–Levy 9

(1994), and of asteroid 253 Mathilde, observed in 1997 by the NEAR probe, suggest low densities and porous constitutions due to their structure (Chapman et al., 1999, Cheng et al., 1999, Davis et al., 1999).

Many arbitrary definitions may be given in general of what a "reaccumulated body" is, depending on the amount of mass contributed by the minor fragments with respect to that of the largest remnant resulting from the breakup. Strictly speaking, we could consider as a reaccumulated body any fragment coming from a shattering event on which a single pebble had softly landed attracted by its gravitational field. Of course, that would provide little information about the structure of the asteroids wandering in the asteroid belt and of the Near Earth Asteroids. Among the many possible arbitrary definitions, we have selected the following simple one: we consider a body to be reaccumulated if the total mass of the reaccreted minor fragments is greater than the mass of the largest single fragment M_{LR}, that is if

$$M_{LR} \; < \; \frac{1}{2}M, \tag{14}$$

M being the mass of the whole reaccumulated body. Of course in reality the transition is probably not so sharp: in many instances the impact outcome will be a single large body coated with a layer of smaller reaccreted bodies accounting for less than half of the total mass, but still forming a deep "megaregolith", in other cases the result will be the formation of an aggregate of a few huge (2–3) fragments, as seems to be the case of Toutatis. However, the definition given above appears to us suitable as a first approximation.

There are a few points about reaccumulated bodies that should be stressed in order to distinguish them from monolithic, unshattered objects.

Some laboratory experiments have been performed by D.R.Davis and E.Ryan by impacting pre–shattered targets, that is objects that have been previously fragmented by a primary impact and then glued together with a special, weak glue, simulating gravitational binding. These targets were then re–impacted. Many informations about the physical characteristics of the target — such as the impact strength S_0 — were obtained from the size distribution of the resulting fragments. In this way they estimated that this parameter does not change in a significant way with respect to the case of non–pre–shattered material. No significant correlation between mass and velocity of fragments has been found in this case. On the other hand, no information on other physical parameters like f_{KE} was available from these experiments. Apart from this attempt for looking for differences between the response to impacts on reaccumulated and monolithic bodies, there are some physical reasons that suggest in principle a different behaviour.

Some authors have studied the propagation of shock waves in porous (non–homogeneous) bodies both by analysing experimental outcomes (Love *et al.* , 1993), and by means of hydrocode numerical simulations (Asphaug *et al.* , 1998), with similar conclusions pointing towards difficulties in the propagation itself.

When a monolithic body is shattered by an energetic collision, the shock wave generated at the contact surface travels accross the body exciting the pre–existing flaws, that coalesce and give rise to many different fragments; the shock wave eventually rebounds at the opposite side of the body and subsequently extinguishes (e.g.:

Grady, 1985). Part of the energy liberated in the impact still remains as kinetic energy that is delivered to the fragments (this fraction can be characterized by f_{KE}) to work against gravitational binding energy. The fragments that are aggregated by self–gravity after ejection, fall upon each other in a random way forming an irregular structure with many voids, eventually with a layer of regolith formed by fine debris over the surface. If such an object happens to undergo a subsequent energetic collision we expect that a large amount of damage is produced in the proximity of the impact point, with the appearance of fast ejecta. The generated shock wave is destined to extinguish quite quickly, in fact it shall rebound on the surface of the fragments in which it develops and shall not be able to propagate further in the target: this is a main difference in the response to impacts between monolithic bodies and rubble–piles. (Note that this may not be true if the projectile is larger than the fragments forming the rubble-pile). The fact that the shock wave is aborted implies that the fragments forming the structure of a rubble–pile — excluding the ones very close to the impact point — should not be seriously damaged, in agreement with the experiments by Ryan *et al.* , 1991, so their mass distribution should be more or less the same as before the impact. A large part of the impact energy is then expected to go into a very large number of highly inelastic collisions between the fragments forming the rubble-pile, and into rotations of the fragments themselves that shall scramble the object changing somehow its shape. As a result of this process, a lot of energy is dissipated, and little kinetic energy is going to reach external fragments, which then will not be able to escape the binding energy of the rubble–pile. If this is what happens in this kind of impacts, the dispersion of rubble–piles requires more energetic impacts than the dispersion of unshattered bodies, a conclusion supported also by Love *et al.* , 1993. Following this conjecture, we have chosen to make two different kinds of simulations. Even if the scenario described above looks reasonable (we are still working on a quantitative estimate of this kind of kinetic process), we conservatively chose to consider—at least for the nominal case—all bodies, both rubble–piles and unshattered bodies, to respond to impacts in the same way ($f_{KE} = 0.1$), and we investigated the effect of considering rubble–piles as having a different response, schematically summarized by imposing $f_{KE} = 0.01$.

IV Results

All the simulations reported below have been run considering the full diameter range from 1 m to 1000 km, although we have plotted only the range from 100 m to 1000 km (anyway, no reaccumulation was found to be noticeable at smaller sizes). The mean relative collisional velocity assumed is $V_{rel} = 5.85 \ km/sec$. The simulated time span for the collisional evolution of the asteroid belt is 4.5×10^9 yr, namely the age of the Solar System. In Table 1, we give the scaling laws and parameters for each collisional model we used. As described in Sec. II, each model, except Durda's scaling law, can have two different velocity distributions: the PF distribution, characterised by "r", and the cumulative distribution, characterised by "k". Hence a collisional model will be designated by its number and a subscript (PF or cum) defining the velocity

11

distribution. The time–evolution algorithm uses real asteroidal cros–section and intrinsic collision probabilities (Bottke *et al.* , 1994). For the initial conditions, we have assumed the same moderate-mass population that we had adopted in our earlier works (Campo Bagatin *et al.* , 1994a,b). We refer to those papers, to Davis *et al.* , 1985, 1989, 1994 and to Campo Bagatin, 1998 for a detailed discussion of the general features of the collisional evolution process and its dependence on the starting conditions and the assumed impact response parameters. It is interesting to note that some constraints on the *a priori* unknown parameters can be derived by the observed spin rate distribution of asteroids, besides their size distribution (Davis *et al.* , 1989; Farinella *et al.* , 1985, 1992).

IV.A Case 1: the Strain–Rate scaling law

We compare here the effect of the two velocity distributions. Figure 2 presents the fraction of rubble-piles in the case of strain–rate scaling law (case 1), as a function of diameter of the target. The solid line shows the cumulative velocity distributions, while the dashed line shows PF velocity distributions. The main feature is the large rubble-pile fraction for bodies from a few hundred kilometers down to 10 or 1 km. The upper cutoff is due to the large strength of bodies of that size. In order to have a rubble-pile, according to our definition, the mass of the largest fragment after the collision and before reaccumulation must be less than half the target mass (the reaccumulated body needs to be at least twice as massive as the largest intact fragment), corresponding to what is called a fragmentation. Hence the kinetic energy of the projectile must be larger than $4\pi/3R^3S$, implying a minimum size for the projectile ($R_p \geq R_{p,min} = R(2S/(\rho V_{rel}^2))^{1/3}$). Given the large value of S, the number of available projectiles is quite small, and the probability of shattering the largest targets over the age of the solar system is quite low. In addition, the kinetic energy deposited by a shattering collision grows with target size faster than the binding gravitational potential, hence the kinetic energy available for the fragments is large enough to allow them to escape the gravitational potential. Thus the lack of rubble-piles of large size is due to a deficiency of both fragmentation and reaccumulation. At the small-size cutoff, on the contrary, the velocity distribution plays an important role.

IV.A.1 Cumulative velocity distribution

We first consider the cumulative velocity distribution case. In Fig. 3a, we present the ratio of reaccumulated mass over mass of the largest intact fragment for a critical mass projectile—that is for a projectile large enough to shatter the target—(solid line) and the maximum ratio over different projectile sizes (dashed line). The horizontal dotted line sets the limit for what we call a rubble-pile. Actually, reaccumulation to form a rubble-pile can occur only for targets larger than about 20 km, which corresponds to the smallest size of rubble-piles in Fig. 2. Note that when rubble-piles can form (dashed line above the horizontal dotted line) then impacts by the smallest projectiles capable of shattering the targets can already create them

(the solid line crosses the horizontal dotted line at the same point as the dashed line). These small projectiles are the most numerous, and hence this explains the rather large fraction of rubble-piles obtained in the collisional evolution. In addition, for targets smaller than 100 km, the rubble–pile formed contains more than half the mass of the original target. Hence, it belongs to the same bin than the target, so very few of the formed rubble-piles belong to the bins smaller than ∼20 km. The rubble-piles in these bins, when hit by a larger than critical projectile, would not reaccumulate, and hence would disappear from the population.

IV.A.2   PF velocity distribution

Figure 3b presents the same quantities in the case of PF velocity distribution. In this case, targets down to 1.4 km can be shattered and yet produce a rubble-pile. However, one needs a projectile larger than the critical size to obtain a rubble pile. In Fig. 4, we display the size of the critical projectile (solid line), the size of the smallest projectile that yields a rubble-pile (short-dashed line) and the size of the projectile giving the largest reaccumulation ratio (long-dashed line), as a function of target size. We can see that down to 10-20 km, the size of the smallest impactor that can create a rubble-pile is just slightly larger than the critical shattering impactor (which is just in the next size bin). Hence the number of reaccumulation events is quite significant compared to the number of disruptions. For smaller sizes, the number of projectiles that can create a rubble-pile is less and less significant compared to the number of disruptive projectiles, and the mass of the reaccumulated body becomes a smaller fraction of the target mass. Hence the fraction of rubble-piles decreases below ∼10 km, and remains non-zero even at sizes smaller than 1.4 km, actually down to ∼500 m.

Another major difference with the cumulative velocity distribution is the large gap in size between the reaccumulated body and the largest escaping fragments. In the PF model, the largest fragments are the slowest, and therefore they are the ones that will reaccumulate. Only the rather small fragments can escape. In the cumulative velocity distribution, on the contrary, fragments of every size have the same velocity distribution. Thus for any given fragment size, there is the same fractions of escaping fragments and of reaccumulated fragments. It results then that the size distribution of escaping fragments shows a smaller gap between the reaccumulated body and the largest escaping fragment.

IV.B   Case 2: a shallower mass-velocity relationship

The PF and cumulative velocity distributions can be viewed as the two extremes of a wide spectrum of velocity distributions. For the cumulative distribution, we assume no relation between mass and velocity. For the PF distribution, there is a strict relation between the mass and the velocity of the fragments. Up to now, we have studied the case were the mass-velocity relationship is as steep as the experiments allow. We now consider a PF velocity distribution with a shallower dependance, i.e. a smaller value of the exponent r: $r = 1/13$. In this case, the small fragments

13

tend to have a lower velocity, and thus less kinetic energy than before. Since we did not change the other parameters, there is an excess of kinetic energy to be shared between the largest fragments. So the largest fragments tend to have a larger velocity than before, and most of them would escape the gravitational binding potential. As a result, we expect to have less rubble-piles with to this small value of r than with the former larger value, as can be seen in Fig. 5.

IV.C Case 3: more dissipative rubble-piles

We consider now the case in which rubble-piles have a lower efficiency in delivering kinetic energy to fragments. As explained in Sec. III, rubble-piles are very likely to be at least as resistant to shattering than monolithic objects, but they might be much more resistant to dispersion. The only change in fragmentation model in this case, compared to case 1, is in the f_{KE} coefficient, set to 0.01 for rubble-piles, considered now to be more dissipative.

Figure 6 represents the fraction of rubble-piles. The main difference with the previous case (Fig. 2) is a larger fraction of rubble-piles at sizes smaller than 200 km. The upper cutoff is the same as in case 1, for the same reasons. In the main size range for which rubble-piles are important, their fraction changes from ∼40-60% in case 1 to ∼60-90% in the present case, depending on the reaccumulation model. Due to the small amount of kinetic energy that the fragments can get, when a collision occurs most of them would reaccumulate on the largest one. While monolithic bodies continue to be disrupted by some critical collisions, rubble-piles instead would survive the same collisions; actually, they are shattered by those collisions, but then they reaccumulate to form a body of essentially the same size. In this way their populations grows with time.

At the lowest cutoff size, the cumulative velocity distribution case allows for rubble–piles down to 4 km, that is to sizes five times smaller than for case 1 (20 km). Reaccumulation and creation of rubble-piles is then possible for targets as small as 4 km. At the beginning of the simulation, there is no rubble-pile in the range 4–14 km. Very few rubble-piles are created in this size range by collisions on targets larger than 20 km by larger than critical projectiles. These rubble-piles, on the other hand, are mostly shattered and reaccumulated to roughly the same size; all these processes result in a small population of rubble-piles at this size range.

For the PF velocity distribution case, rubble-piles as small as 500 m can be shattered and reaccumulated. However, here again—as explained in Sec. IV.A.2—for sizes smaller than ∼10 km, this requires projectiles larger than the critical shattering size. Since these projectiles are less numerous than critical ones, the most common outcome of a shattering collision would be the creation of monolithic fragments, smaller than half the target's mass. Then the fraction of rubble-piles is more or less the same—in this size range—for the PF velocity distribution case, in the case of "standard" and low values of f_{KE}.

IV.D Cases 4 and 7: weak bodies

We consider now "weaker" bodies, for which the strain–rate scaling law with $S_0 = 3 \cdot 10^5$ J/m^3 and the hydrocode scaling law representative of basalt with $S_0 = 8.22 \cdot 10^6$ J/m^3 are considered. The main difference between the PF and the cumulative velocity distribution that we have seen so far, i.e. a noticeable fraction of rubble-piles that extends to smaller sizes in the former case than in the latter, holds for the cases of weaker bodies that we have tested. In these cases, we will study only the cumulative velocity distribution, since it gives smooth final populations. In the PF cases, rubble-piles are simply also present at sizes an order of magnitude smaller.

The fractions of rubble-piles for both cases 4 and 7 are shown on Fig. 7. This fraction is larger than for case 1 (Fig. 2), and rubble-piles are present at smaller and larger sizes. At all sizes, targets can be shattered by smaller projectiles than in case 1, that is with less kinetic energy. Hence the fragments created in the collisions are less likely to escape, even for collisions by critical projectiles. Targets larger than 200 km can therefore be shattered and reaccumulated, as well as the ones smaller than 10 km. The smaller size of critical projectiles increases their number for a given target size, thus favouring the creation of rubble-piles between 10 and 200 km, as compared to case 1. Here, the strength in the strain–rate scaling law is 10 times smaller than the one displayed on Fig. 1. So it becomes smaller than for hydrocode scaling at sizes smaller than about 5 km. It follows that rubble-piles exist only down to ~4 km in the case of hydrocode scaling, while they exist down to ~2 km in the case of strain–rate scaling.

IV.E Cases 5 and 6: Strong bodies

We consider now the two cases in which we assume very "strong" targets. One can see on Fig. 1 that multiplying the strain–rate scaling strength by 10 makes it very close to the energy scaling strength. So we expect to get rather similar results in both cases. In the present cases, as opposed to the previous ones, it is rather difficult to create rubble-piles. The energy required to shatter a given target is 10 to 100 times larger than before, and the critical impacts deliver a lot of kinetic energy to the fragments, while the largest fragments are rather large, making it difficult to reaccumulate enough mass to form what we call a rubble-pile. Actually, for the cumulative distribution velocity cases, there are essentially no rubble-piles (fraction less than $3 \cdot 10^{-3}$) at any size.

In the PF velocity distribution cases, rubble-piles can still be created, albeit in a narrower size-range, as can be seen in Fig. 8. The largest rubble-piles are about half the size as those in case 1, while the smallest ones are about twice as large, around 1 km. The maximum fraction of rubble-piles is about 40%, between 20 and 50 km.

IV.F Case 8: Durda *et al.* scaling law

We finally consider the scaling law proposed by Durda *et al.* , 1998 that they obtained by fitting the "debiased" observed size distribution of asteroids for bodies

15

larger than a few kilometers. A note of caution is necessary here. First, as mentioned in Sec. II, they derived a scaling law for the critical specific energy for dispersal, while our model requires the critical energy for shattering. This led us to define a varying f_{KE} as a function of the size of the target (Eq. 10). Second, the details of fragmentation models are different (see Durda and Dermott, 1997 and Petit and Farinella, 1993). For consistency reasons, we only considered the cumulative velocity distribution case, with $k = 9/4$. In Fig. 9, we have plotted Eq. 10 with this value of k, and Q_D^* given by Eq. 9 and V_{esc} by Eq. 12. This curve is characterized by a maximum of 0.6 around 6-7 km and significant decreases for both smaller and larger targets.

For the creation of rubble-piles, we must consider three different regimes. First, for the large targets, larger than ∼200 km, the strength is very large, so large that almost no projectile can shatter targets of that size. In case shattering occurs, the kinetic energy available is so large that enough fragments escape to avoid creating a rubble-pile, despite the decrease of f_{KE} from 0.1 to 0.015. For intermediate size targets, between 1 and 200 km, the strength is in the same range as in the previous cases. However, f_{KE} is large at that size, and the kinetic energy of the fragments allow them to escape. Finally, for smaller targets, even though the strength is quite small and f_{KE} is small also, the gravitational binding energy decreases too fast to allow for much reaccretion. In addition, the collisional lifetime of bodies of that size is quite small, due to the small strength, and most of the fragments are actually regenerated by fragmentation of larger targets. These freshly created fragments appear at first as monolithic bodies.

As noted above, f_{KE} reaches unrealistically low values at small sizes, and maybe even at large sizes. This results from the requirement that only half the mass of the target has a kinetic energy large enough to escape (Eq. 10). However, it may turn out that the amount of kinetic energy of the fragment is larger than the minimum required by $f(> V_{esc}) > 1/2$. This is the case, for example, for small targets where the critical shattering energy is quite large compared to the gravitational binding energy, thus yielding to $V_{min} > V_{esc}$. So a more realistic definition of f_{KE} could be:

$$f_{KE} = \max\left(\frac{k}{k-2} \, 2^{-2/k} \, \frac{v_{esc}^2}{Q_D^*}, 0.1 \right). \tag{15}$$

In this case, Q_S^* is computed from the first part of Eq. 13. However, the ratio

$$\frac{\frac{1}{f_{KE}} \, 0.411 \, \frac{2\,G\,M_T}{D}}{Q_D^*}$$

never exceeds ∼0.05, even when f_{KE} has no lower limit, and it can be much smaller than that if we use Eq. 15. Hence the strength is mostly unchanged, and there is no reaccumulation of rubble-piles (according to our definition). In all the simulations performed using Durda *et al.* scaling law, the maximum reaccumulation is about 20-25% of regolith on top of the largest fragment.

Here we give a brief explanation as why we think that Durda *et al.* , 1998 is not totally self–consistent. The collisional evolution model used is that work

is essentially the one described in Durda and Dermott, 1997 (hereafter D & D) which seems to suffer from some unphysical assumptions. D & D use a power-law differential size distribution for the fragments resulting from a collision between a target and a projectile larger than D_{min} determined by their eq. (9)

$$dN = BD^{-p}dD. \tag{16}$$

They make a confusion in the definition of p. They first give its value as being slightly larger than 2.5 (eq. (11), page 149), and then as being slightly larger than 3.5 (page 155). The later value actually corresponds to the differential size distribution exponent, while the former corresponds to the cumulative size distribution. Their eq. (12) relates the differential size distribution exponent to the fractional size of the largest remnant b. So the appropriate range of values for p is really 3.5 to 4. In their simulations, they fix p, hence fixing b. So the size of the largest fragment is fixed with respect to the size of the target, regardless of the kinetic energy of the collision. Finally, in D & D, the reaccumulation is neglected. Actually, they don't consider the reaccumulation to be a different process from shattering. In a shaterring followed by reaccumulation, one would first have a power-law size distribution of fragments, and then, some of them (which ones depend on the mass-velocity relationship) would reaccrete on the largest fragment. Hence the distribution would consist of a very large fragment (the rubble pile) and a power-law distribution of smaller fragments, with a gap in between. In Durda *et al.* , 1998, the only change is to define the minimum kinetic energy required as:

$$E_{min} = MQ^*. \tag{17}$$

The largest remnant can therefore be either a monolithic fragment or a rubble pile. But the size distribution is always a power-law with a fixed exponent, starting from that largest remnant. In addition, the values they use for p (2.82 and 2.47) seem to be cumulative size distribution exponents, which is not clearly stated, and contrary to the expected differential size distribution exponent.

IV.G Benz and Asphaug, 1999 scaling law

During the review process, we have learnt about the new scaling laws proposed by Benz and Asphaug, 1999 and which was not yet published at the time we performed all the calculations presented in the present paper. Here again, as in Durda *et al.* , 1998, the authors give Q_D^* as a function of the size of the target. In addition, all the other assumptions that we make about the outcome of a collision are not present in that work, neither explicitly nor implicitly. Therefore, it is not really relevant to use Benz and Asphaug scaling law in our model. However, we run a simulation for a basaltic target, and defining Q_S^* according to Eq. 13, f_{KE} being given by Eq. 15. For reasons similar to those presented in Durda *et al.* case, we found no rubble–pile satisfying our defintion.

V Conclusions

Our results show that reaccumulation is probably commonplace (albeit not "universal") for main–belt asteroids in the intermediate diameter range from ~10 to 200 km. In this range the fraction of rubble-piles goes from about 30% to 100%, depending on physical parameters. This may extend to smaller or larger sizes, namely from 0.5-1 to 500 km, depending on the collisional response parameters. The upper cutoff varies mainly with the assumed scaling law for the impact strength S, allowing for larger targets to reaccumulate after collisions if they are weak. Rubble-piles can exist in a noticeable fraction down to ~0.5-1 km if we assume a fixed mass-velocity relationship such as the one in Eq. 5. For a probably more realistic velocity distribution, such as the one given in Eq. 6, the smallest rubble-piles have a diameter of 3 to 15 km, depending on the strength of the targets. When assuming weak targets, such as with the hydrocode scaling law, or the strain–rate scaling law with $S_0 = 3 \cdot 10^5$ J/m^3, the fraction of rubble-piles exceeds 90% from 5 to 300 km. On the opposite, for strong targets, the formation of rubble-piles becomes more difficult. Actually, no rubble-pile is formed with the cumulative velocity distribution, for the energy scaling and the strain–rate scaling with $S_0 = 3 \cdot 10^7$ J/m^3, and it does not exceed 40% for the PF velocity distribution. When applying our algorithm to Durda *et al.*, 1998 scaling law, and changing from Q_D^* to Q_S^*, we obtain no rubble–pile according to our definition (largest fragment less than half the mass of the reaccumulated body).

The simulations performed in this work show that the mass-velocity dependence is a main feature of the physics of collisions at high velocity. Caution has to be taken when considering this relationship in a very schematic way, especially for small values of the exponent of the power law. In fact, neglecting the dispersion of data actually present in all laboratory experiments on this issue, may lead to wrong conclusions. We find a very strong dependence of the reaccumulation fraction, at any given size, on the mass–velocity relationship. Considering very shallow mass–velocity relationships, leads to very small fractions of rubble–piles, below 20% for $r = 1/13$ around 100 km (Fig. 5), and negligible at other size ranges; close to 0% at all sizes for $r = 0$. We believe that this is only an effect of the way the mass–velocity relationship is modelled. Experimental results for the mass and velocity of fragments show that data are widely dispersed, and that they are loosely distributed about some power–law relationship. If we schematically assume a mathematical expression like the one given in the text for that relationship, we are forcing every fragment of mass m$_i$ to have a given velocity v$_i$. In the case in which the relationship between these two quantities is very shallow, that is when r is very small or, as an extreme case, when it is zero, then all fragments would have almost the same speed. That speed may be smaller or larger than the escape velocity from the body. In the case with $r = 1/13$ we find that most of the fragments have velocities larger than the escape velocity, and we obviously end up with almost no reaccumulation. In this way we introduce an artificial bias into the process, that shows up to be relevant at very small values of the exponent r. More laboratory experiments are indeed needed to better bound this relationship. It is clear now that having *no* relationship

between mass and velocity of fragments (that is assuming a cumulative model) *is not* at all the same thing as having a mass–velocity relationship with a null exponent. It seems obvious that both PF and cumulative models are two "extreme" ways to model the reaccumulation process; in the former case the mass-velocity relationship is taken into account "too seriously", while in the latter it is completely neglected. Is the truth somewhere in between? That is probably the case, and we intend to refine the modelling of the phenomenon in future work.

Another interesting result of our simulations is that if we wish to model in a realistic way the collisional evolution of asteroidal systems, we should not neglect the physical differences between reaccumulated and unshattered bodies. We have summarized this differences just focusing on the response to impacts in terms of the different fraction of kinetic energy f_{KE}, (f_{KE}=0.1 for unshattered objects, and f_{KE}=0.01 for rubble–piles) delivered to the fragments in the two cases, and we have found that this implies a detectable difference in the population of asteroids at the end of the collisional evolution, and that the fraction of reaccumulated asteroids is noticeably higher.

Both the facts that rubble-piles may be harder to disrupt compared to unshattered objects, and that they may not be unusual also at km-sizes, may have direct consequences on future deviation/destruction strategies regarding the risk of impact events on Earth by asteroids.

Acknowledgments

References

ASPHAUG, E. AND BENZ, W. 1994. Density of comet Shoemaker-Levy 9 deduced by modelling breakup of the parent 'rubble pile'. *Nature* **370,** 120–124.

ASPHAUG, E., OSTRO, S.J., HUDSON, R.S., SCHEERES, D.J. AND BENZ, W. 1998. Disruption of kilometre-size asteroids by energetic collisions. *Nature* **393,** 437–440.

BOTTKE, W.F., NOLAN, M.C., GREENBERG, R. AND KOLVOORD, R.A. 1994. Velocity Distributions among Colliding Asteroids. *Icarus* **107,** 255–268.

CAMPO BAGATIN, A. 1998. *Ph. D. Thesis*, ISBN 84–3703447–7, University of Valencia, Spain

CAMPO BAGATIN, A., CELLINO, A., DAVIS, D.R., FARINELLA, P. AND PAOLICCHI, P. 1994a. Wavy size distributions for collisional systems with a small-size cutoff. *Planet. Space Sci.* **42,** 1079–1092.

CAMPO BAGATIN, A., FARINELLA, P. AND PETIT, J-M. 1994b. Fragment ejection velocities and the collisional evolution of asteroids. *Planet. Space Sci.* **42,** 1099–1107.

CHAPMAN, C.R., MERLINE, W.J. AND THOMAS, P. 1999. Cratering on Mathilde. *Icarus* **140,** 28–33.

CHENG, A.F. AND BARNOUIN, O.S. 1999. Giant Craters on Mathilde. *Icarus* **140,** 34–48.

DAVIS, D.R. 1999. The Collisional History of Asteroid 253 Mathilde. *Icarus* **140,** 49–52.

DAVIS, D.R., CHAPMAN, C.R., WEIDENSCHILLING, S.J. AND GREENBERG, R. 1985. Collisional History of Asteroids: Evidence from Vesta and the Hirayama Families. *Icarus* **62,** 30–53.

DAVIS, D.R., WEIDENSCHILLING, S.J., FARINELLA, P., PAOLICCHI, P. AND BINZEL, R.P. 1989. Asteroid collisional history: effects on sizes and spins. in *Asteroids II,* (R.P. Binzel, T. Gehrels and M.S. Matthews, Eds.) The University of Arizona Press, pp. 805–826.

DAVIS, D.R., RYAN, E.V. AND FARINELLA, P. 1994. Asteroid collisional evolution: results from current scaling algorithms. *Planet. Space Sci.* **42,** 599–610.

DOHNANYI, J.W. 1969. Collisional Model of Asteroids and Their Debris. *J. Geophys. Res.* **74,** 2531–2554.

DURDA, D.D. AND DERMOTT S.F. 1997. The Collisional Evolution of the Asteroid Belt and Its Contribution to the Zodiacal Cloud. *Icarus* **130,** 140–164.

DURDA, D.D., GREENBERG, R. AND JEDICKE, R. 1998. Collisional Models and Scaling Laws: A New Interpretation of the Shape of the Main-Belt Asteroid Size Distribution. *Icarus* **135,** 431–440.

FARINELLA, P. AND DAVIS, D.R. 1992. Collision Rates and Impact Velocities in the Main Asteroid Belt. *Icarus* **97,** 111–123.

FARINELLA, P., PAOLICCHI, P. AND ZAPPALÁ, V. 1982. The Asteroids as Outcomes of Catastrophic Collisions. *Icarus* **52,** 409–433.

FARINELLA, P., PAOLICCHI, P. AND ZAPPALÀ, V. 1985. Original abundance of asteroids from their present rotational properties. *Mon. Not. R. Astron. Soc.* **216,** 565–570.

FARINELLA, P., DAVIS, D.R., PAOLICCHI, P., CELLINO, A. AND ZAPPALÀ, V. 1992. The collisional lifetime of asteroid 951 Gaspra. *Astron. Astrophys.* **257,** 329–330.

FARINELLA, P., GONCZI, R., FROESCHLÉ, CH. AND FROESCHLÉ, C. 1993. The Injection of Asteroid Fragments into Resonances. *Icarus* **101,** 174–187.

FUJIWARA, A. 1980. On the Mechanism of Catastrophic Destruction of Minor Planets by High-Velocity Impact. *Icarus* **41,** 356–364.

GIBLIN, I. 1998. New data on the velocity-mass relation in catastrophic disruption. *Planet. Space Sci.* **46,** 921–928.

GIBLIN, I., MARTELLI, G., SMITH, P.N., CELLINO, A., DI MARTINO, M., ZAPPALÀ, V., FARINELLA, P. AND PAOLICCHI, P. 1994. Field Fragmentation of Macroscopic Targets Simulating Asteroidal Catastrophic Collisions. *Icarus* **110,** 203–224.

GRADY, D. 1985. The mechanics of Fracture Under High-Rate Stress Loading. in *Mechanics of Geomaterials,* Wiley & Sons Ltd., pp. 129–156.

HOLSAPPLE, K.A. 1994. Catastrophic Disruptions and cratering of Solar System Bodies: a Review and New results. *Planet. Space Sci.* **42,** 1067–1078.

HOUSEN, K.R. AND HOLSAPPLE, K.A. 1990. On the Fragmentation of Asteroids and Planetary Satellites. *Icarus* **84,** 226–253.

HOUSEN, K.R. AND HOLSAPPLE, K.A. 1999. Scale Effects in Strength Dominated Collisions of Rocky Asteroids. *Icarus* **142,** 21–33.

HOUSEN, K.R., SCHMIDT, R.M. AND HOLSAPPLE, K.A. 1991. Laboratory Simulations of Large Scale Fragmentation Events. *Icarus* **94,** 180–190.

LOVE, S.G. HÖRZ, F. AND BROWNLEE, D.E.. 1993. Target Porosity Effects in Impact Cratering and Collisional Disruption. *Icarus* **105,** 216–224./

MELOSH, H.J. AND RYAN, E.V. 1997. Asteroids: Shattered but Not Dispersed. *Icarus* **129,** 562–564.

NAKAMURA, A. AND FUJIWARA, A. 1991. Velocity Distribution of Fragments Formed in a Simulated Collisional Disruption. *Icarus* **92,** 132–146.

NAKAMURA, A., SUGUIYAMA, K. AND FUJIWARA, A. 1992. Velocity and Spin of Fragments from Impact Disruptions. I. An Experimental Approach to a General Law between Mass and Velocity. *Icarus* **100,** 127–135.

PETIT, J-M. AND FARINELLA, P. 1993. Modelling the outcomes of high-velocity impacts between small solar system bodies. *Celest. Mech.* **57,** 1–28.

RYAN, E.V., HARTMANN, W.K. AND DAVIS, D.R. 1991. Impact Experiments 3: Catastrophic Fragmentation of Aggregate Targets and Relation to Asteroids. *Icarus* **94,** 283–298.

21

VEDDER, J.D. 1997. Main Belt Asteroid Collision Probabilities and Impact Velocities. *Icarus* **131,** 283–290.

WEISSMAN, P.R. 1986. Are cometary nuclei primordial rubble piles ?. *Nature* **320,** 242–244.

WHIPPLE, F.L. 1998. Note on the structure of comet nuclei. *Planet. Space Sci.* **47,** 301–304.

WILSON, L., KEIL, K. AND LOVE, S.G. 1999. The internal structures and densities of asteroids. *Meteoritics & Planet. Sci.* **34,** 479–483.

Figure captions

Figure 1: Strength versus diameter of the target according to the different scaling laws considered in the simulations. The strength is the critical energy per unit volume needed to shatter a target so that the largest fragment has half the mass of the inital target.

Figure 2: Fraction of rubble-piles (reaccumulated asteroids with mass larger than twice the mass of the largest fragment) versus diameter at the end of collisional evolution. This plot corresponds to the case 1, strain–rate scaling, for both cummulative (solid line) and PF (dashed line) velocity distribution. The curves are somewhat irregular due to the stochastic nature of the collisional process. Depending on the size of the critical projectile compared to the center of the corresponding bin, the largest fragment can vary a lot, and also its ability to reaccrete material.

Figure 3: Ratio of mass of reaccumulated fragments over mass of the largest fragment after shattering, as a function of target size, for case 1. Solid line corresponds to an at least critical projectile (belonging to the smallest bin that is large enough to shatter the target), and dashed line to the maximum reaccumulation when varying the projectile mass. (a) Cumulative velocity distribution. (b) PF velocity distribution.

Figure 4: Projectile diameter versus target diameter for the critical projectile (solid line), the smallest projectile capable of creating a rubble-pile (short-dashed line) and for the maximum reaccumulation (long-dashed line) for case 1 and PF velocity distribution, as a function of target size. The two dashed curves stop when there is no more reaccumulation. The roughness of the curve is due to the discreteness of the size bins (size ratio of $2^{1/3}$), preventing to find the exact critical values.

Figure 5: Same as Fig. 2, but for PF velocity distribution and $r = 1/13$.

Figure 6: Same as Fig. 2, but for more dissipative rubble-piles, i.e. $f_{KE} = 0.01$ for rubble-piles.

Figure 7: Same as Fig. 2, but for cases 4 (solid line) and 7 (dashed line).

Figure 8: Same as Fig. 2, but for cases 5 (solid line) and 6 (dashed line).

Figure 9: f_{KE} as a function of target diameter, as derived from Durda *et al.* best fit for Q_D^*

Case	Scaling law	S_0 (J/m³)	f_{KE}	r	k
1	Eq. 2	$3\ 10^6$	0.1	1/6	2.25
2	Eq. 2	$3\ 10^6$	0.1	1/13	-
3	Eq. 2	$3\ 10^6$	0.1/0.01	1/6	2.25
4	Eq. 2	$3\ 10^5$	0.1	1/6	2.25
5	Eq. 2	$3\ 10^7$	0.1	1/6	2.25
6	Eq. 1	$3\ 10^6$	0.1	1/6	2.25
7	Eq. 3	$8.22\ 10^6$	0.1	1/6	2.25
8	Eq. 13	-	Eq. 10	-	2.25

Table 1: The physical parameters used in the simulations are summarized here. The material density $\rho = 2500$ kg/m³ and the self–compression coefficient $\alpha = 100$. For each case we list here the scaling law, the material strength S_0, anelasticity coefficient f_{KE}, mass–velocity exponent r, and cumulative velocity distribution exponent k, when applicable.

Figure 1; A. Campo Bagatin et al.

Strength scaling laws
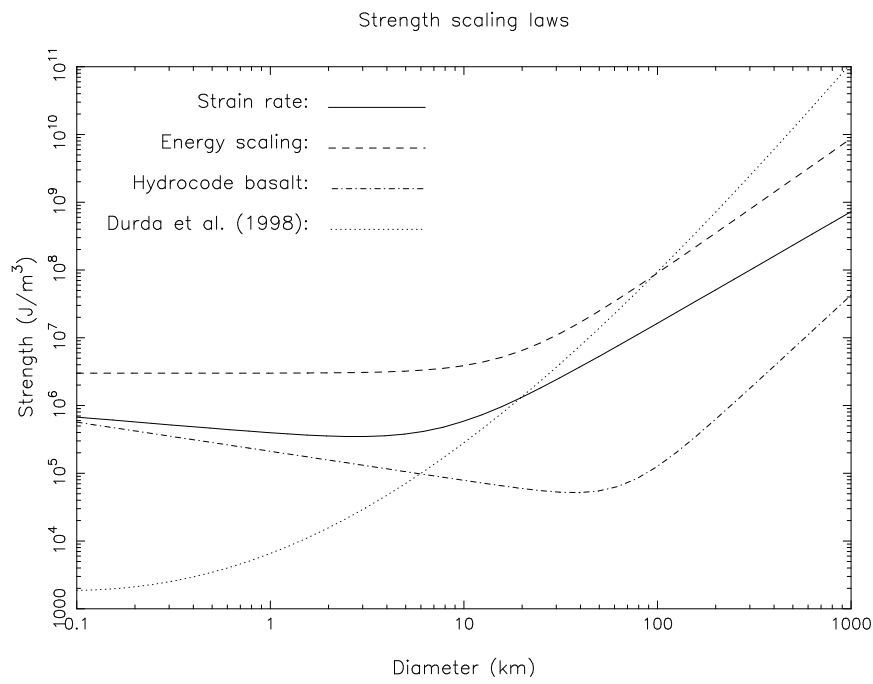
Figure 2; A. Campo Bagatin et al.
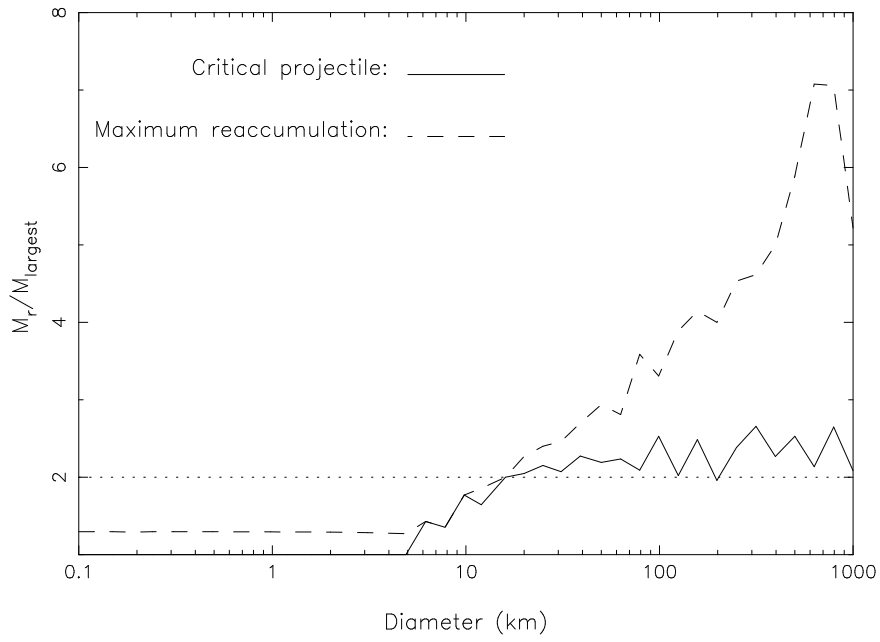
Case 1: Strain rate scaling law
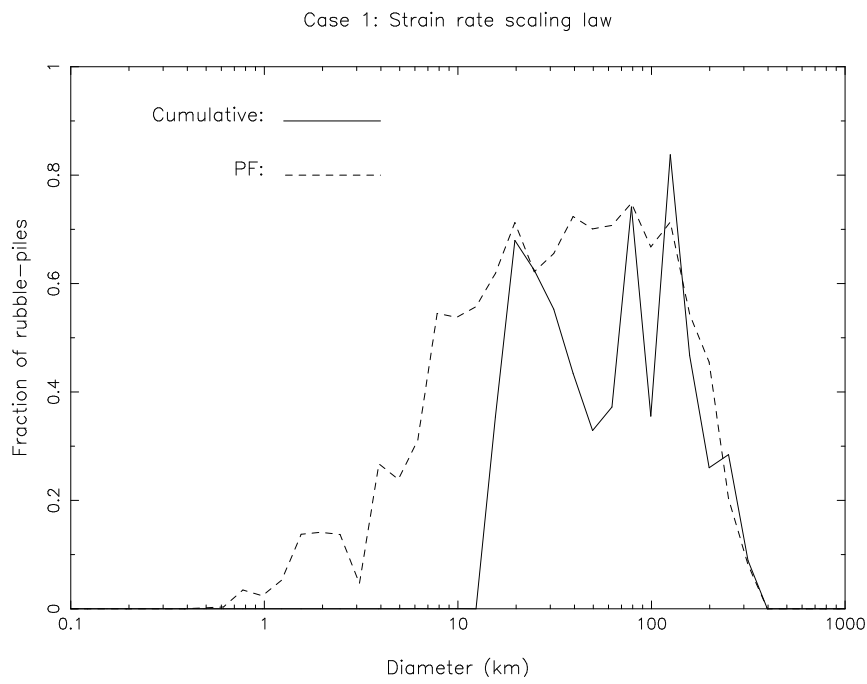
Figure 3; A. Campo Bagatin et al.

(a). Case 1: Cummulative velocity distribution

(b). Case 1: PF velocity distribution

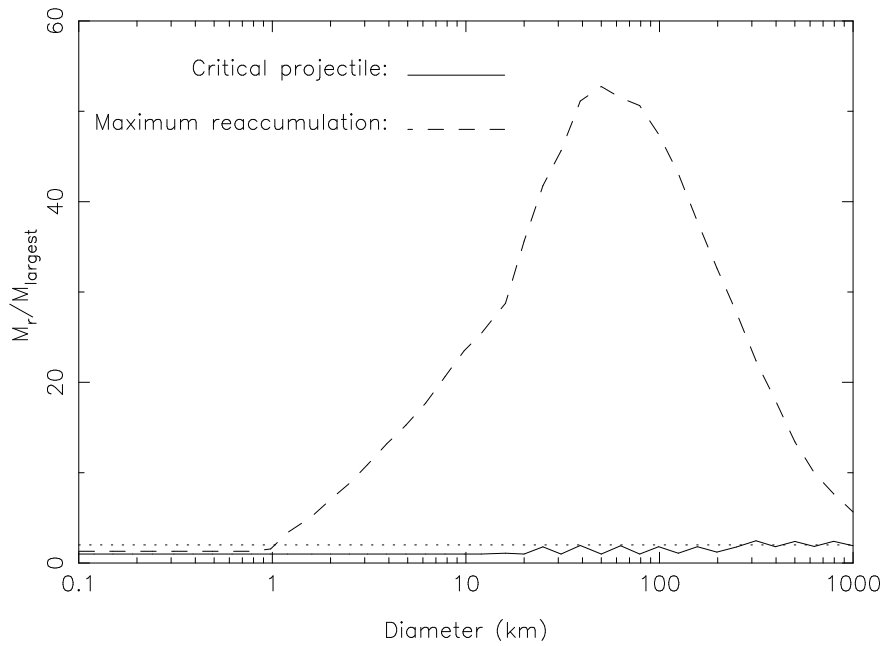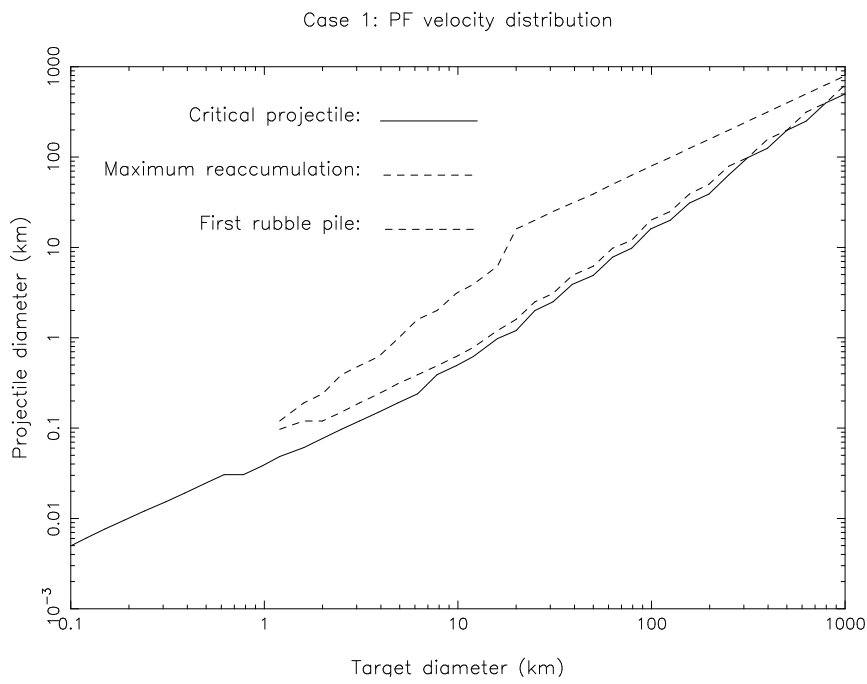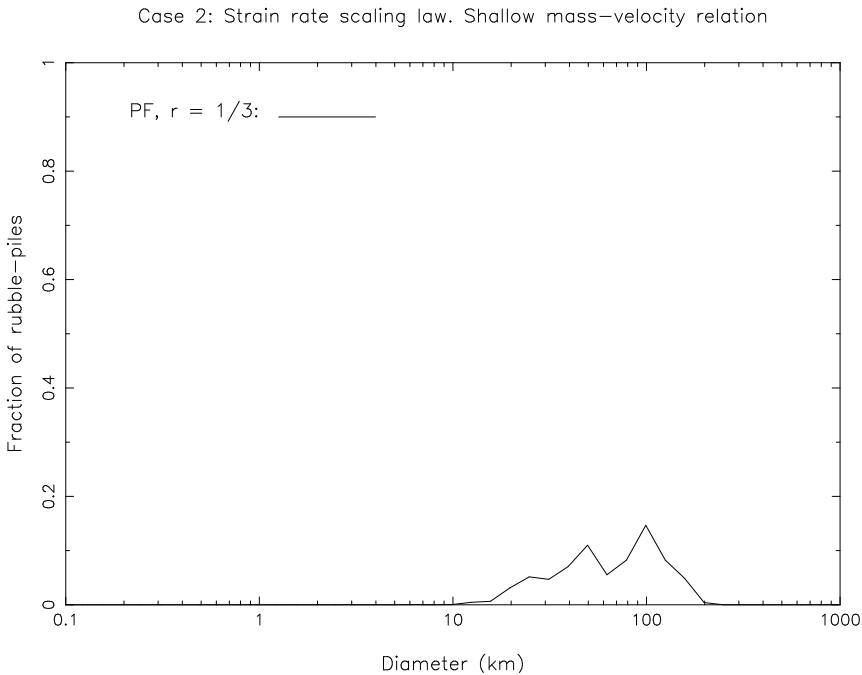Figure 4; A. Campo Bagatin et al.

Case 1: PF velocity distribution

Figure 5; A. Campo Bagatin et al.

Case 2: Strain rate scaling law. Shallow mass−velocity relation

29

Figure 6; A. Campo Bagatin et al.

Case 3: Strainrate scaling law, low f_{KE} rubble−piles
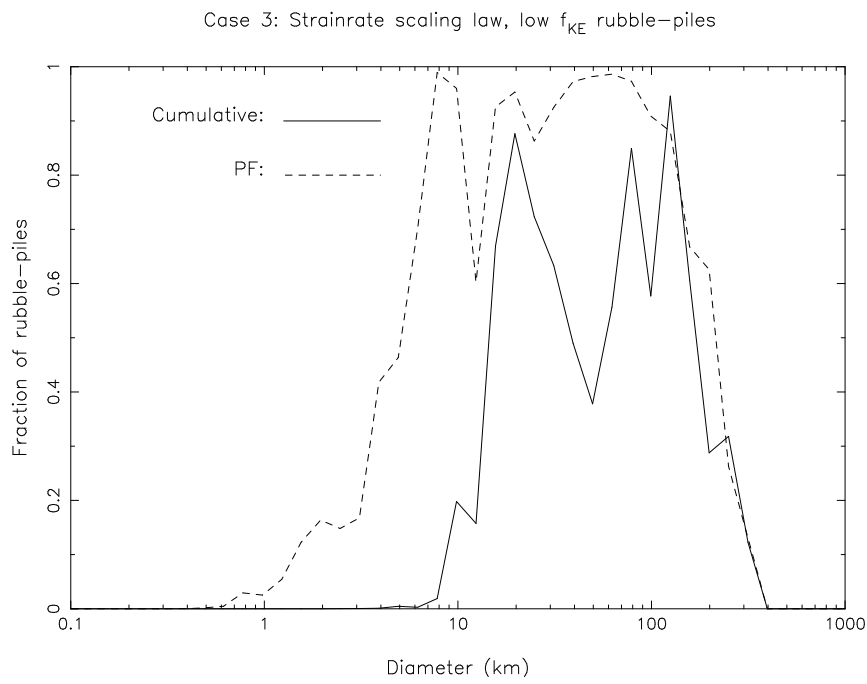
Figure 7; A. Campo Bagatin et al.

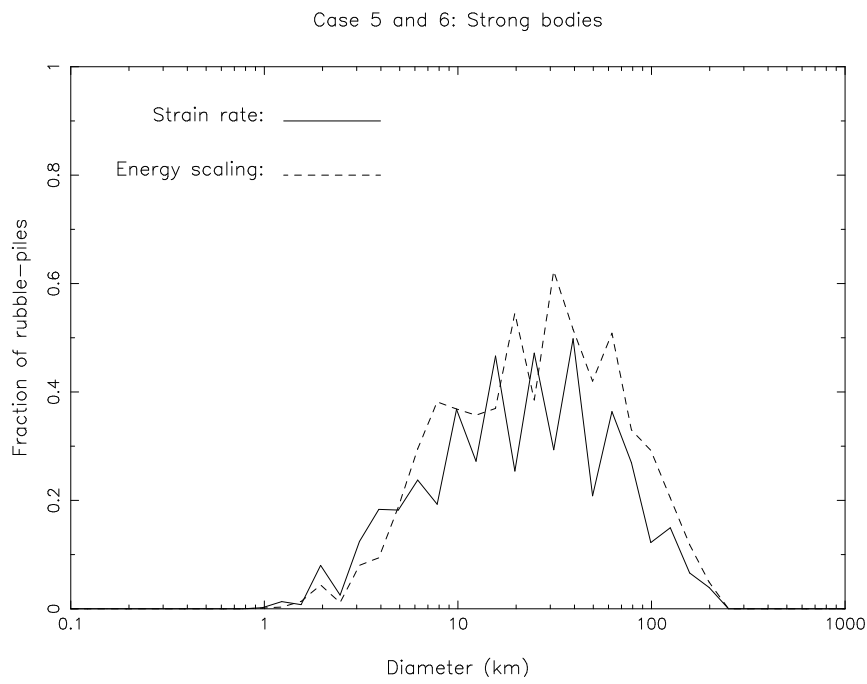Case 4 and 7: Weak bodies
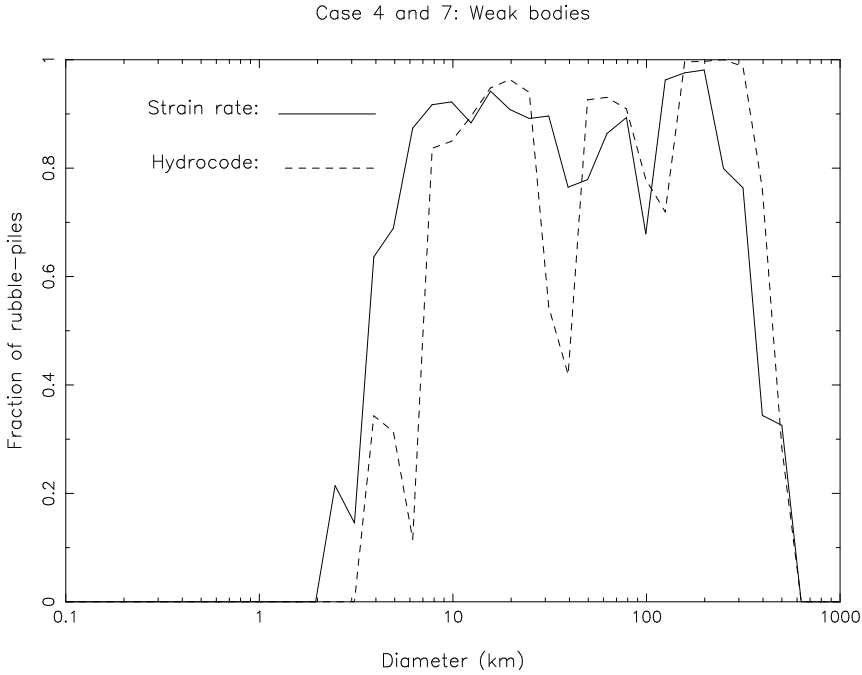
Figure 8; A. Campo Bagatin et al.

Case 5 and 6: Strong bodies

Figure 9; A. Campo Bagatin et al.

Durda et al. scaling law. k = 9/4